Stable gravastars: Guilfoyle's electrically charged solutions

Ayan Banerjee[1;1)] J. R. Villanueva[2;2)] Phongpichit Channuie[3;3)] Kimet Jusufi[4;4)]

[1] Department of Mathematics, Jadavpur University, Kolkata-700032, India
[2] Instituto de Física y Astronomía, Facultad de Ciencias, Universidad de Valparaíso, Gran Bretaña 1111, Valparaíso, Chile
[3] School of Science, Walailak University, Nakhon Si Thammarat, 80160 Thailand
[4] Physics Department, State University of Tetovo, Ilinden Street nn, 1200, Macedonia

Abstract: Compelling alternatives to black holes, namely, gravitational vacuum stars (*gravastars*), which are multilayered compact objects, have been proposed to avoid a number of theoretical problems associated with event horizons and singularities. In this work, we construct a spherically symmetric thin-shell charged gravastar model where the vacuum phase transition between the de Sitter interior and the external Reissner–Nordström spacetime (RN) are matched at a junction surface, by using the cut-and-paste procedure. Gravastar solutions are found among the Guilfoyle exact solutions where the gravitational potential W^2 and the electric potential field ϕ obey a particular relation in a simple form $a(b-\epsilon\phi)^2+b_1$, where a, b and b_1 are arbitrary constants. The simplest ansatz of Guilfoyle's solution is implemented by the following assumption: that the total energy density $8\pi\rho_m+\frac{Q^2}{r^4}$ is constant, where $Q(r)$ is the electric charge up to a certain radius r. We show that, for certain ranges of the parameters, we can avoid the horizon formation, which allows us to study the linearized spherically symmetric radial perturbations around static equilibrium solutions. To lend our solution theoretical support, we also analyze the physical and geometrical properties of gravastar configurations.

Keywords: gravastar, Guilfoyle exact solutions, stability analysis

PACS: 04.20.Jb **DOI:** 10.1088/1674-1137/42/11/115101

1 Introduction

The final state of a star's gravitational collapse can lead to the formation of different objects such as neutron stars, white dwarfs, black holes and naked singularities [1–5]. This end-state of collapse is a widely accepted field of research in the scientific community from many perspectives, both theoretical and observational. However, classical general relativity suffers from some severe theoretical problems. One problem is related to the paradoxical features of black holes and naked singularities. In order to resolve these issues, the idea of the existence of compact objects without event horizons has recently been proposed, the so-called *gravastar*: an alternative to black holes [6–8]. Moreover, some interesting articles have been published. Within these models, a massive star in its final stages could end its life as a gravastar that compresses matter within the gravitational radius $r_s = 2\ \mathrm{GM/c^2}$, i.e., very close to the Schwarzschild radius, but with no singularity or event horizon. In this situation, the quantum vacuum fluctuations are expected to play a non–trivial role at or near the event horizon. Based on the gravastar framework, the solutions of Mazur and Mottola's gravastar scenario describe five layers of the gravastar, including two thin shells. The de Sitter geometry in the interior, with an equation of state (EOS) $p = -\rho$, matches to an exterior Schwarzschild vacuum geometry. Between the interior and exterior geometry, there is a finite–thickness shell comprised of stiff fluid matter with EOS $p = +\rho$. Due to their extreme compactness, however, it would be very difficult to distinguish gravastars from black holes. As an extension of the Mazur–Mottola model and for physical reasons, Visser and Wiltshire [9] reduced the number of thin shells from 5 layers to 3 layers with a continuous layer of finite thickness, where the phase transition layer was replaced by a single spherical δ-shell. In the model, by the definition of the gravastar, a de-Sitter spacetime was matched to a Schwarzschild exterior solution at a junction surface with surface stresses σ and $\mathcal{P}$. Moreover, the authors provided full dynamic stability against spherically symmetric perturbations by using the Israel

Received 7 May 2018, Revised 5 August 2018, Published online 26 September 2018

1) E-mail: ayan_7575@yahoo.co.in
2) E-mail: jose.villanueva@uv.cl
3) E-mail: channuie@gmail.com
4) E-mail: kimet.jusufi@unite.edu.mk

thin shell formalism [10] in terms of an effective energy equation. This simplified form of gravastar structure has also motivated a number of physicists to consider different types of vacuum geometries in the interior and exterior. Among these models, Bilić and his collaborators have shown how a gravastar structure can form a Born–Infeld scalar field [11] and a non-linear electrodynamic gravastar [12]. In Ref. [13], gravastar solutions have been studied by replacing the δ–shell with a continuous stress-energy tensor from the asymptotically de Sitter interior to the exterior Schwarzschild solution. Moreover, an electrically charged gravastar has been studied by solving the Einstein–Maxwell field equations in the asymptotically de Sitter interior [14], whereas a charged gravastar admitting conformality was constructed in Ref. [15]. In the same vein, Chan et al. [16] have studied radiating gravastars by considering Vaidya exterior spacetime. However, it was shown that the interior de Sitter spacetime may also be replaced by considering a solution governed by the dark energy equation of state, $\omega=p/\rho$ where $\omega<-1/3$ [17]. Furthermore, much effort has been made to investigate the properties of gravastars in the context of alternative scenarios. These were considered in Refs. [18–22].

An interior regular charged perfect fluid solution can not only contribute to a better understanding of the structure of spacetime, but physically it also offers many new and interesting solutions. A static solution around a spherically non-rotating charged body was stimulated by the work of Reissner and Nordström [23]. Almost at the same time, Hermann Weyl [24, 25] studied vacuum general relativity and electromagnetism, which together established a relation between the metric component g_{tt} and the electric potential ϕ. A further discussion about this relation appeared in 1947 when Majumdar [26] generalized this result to systems without spatial symmetry. Regarding this point of view, further development on Weyl's work was examined much later by Guilfoyle [27]. He considered charged fluid distributions in which the interior of these solutions is characterized by the relation between the gravitational and the electric potential, which are functionally related to each other via $W=W(\phi)$. Here W is parametrized by $W^2=a(b-\epsilon\phi)^2+b_1$, where a, b and b_1 are arbitrary constants, and $\epsilon=\pm$. Specifically, this relation generalizes the common Weyl relation, when $a=1$, and the extension of this concept was discussed by Lemos and Zanchin [28]. Here they obtained a relationship between various fields and matter quantities. The authors also studied quasiblack holes such as frozen stars [29], and found regular black holes for the Guilfoyle exact solutions [30] with the discussion of their physical relevances. In addition, Lemos and Zanchin [31] applied the method to study relativistic charged spheres, and showed that when the central pressure goes to infinity Guilfoyle's stars also obey the Buchdahl-Andréasson bound. Moreover, regarding the Weyl and Weyl–Guilfoyle relations, general relativistic charged fluids with non–zero pressure turned out to be an important cornerstone for addressing and discovering new solutions. Thus, it is interesting to embark on a study of the Guilfoyle model with the presence of electrically charged matter. We expect that gravastar solutions should be found within a certain range of the parameters of the model.

The outline of the paper is as follows. In Section **2**, we present Guilfoyle's exact solutions with the ansatz $W^2=a(b-\epsilon\phi)^2+b_1$. In Section **3**, the basic equations for spherically symmetric spacetime with electrically charged perfect fluid matter distribution are written, satisfying a particular Weyl–Guilfoyle relation, and we discuss the interior and exterior solutions with appropriate boundary conditions in Section **4**. In Section **5**, we briefly review some gravastar models. In Section **6**, we present the basic setup for matching the two distinct spacetimes and obtaining models of the thin shell gravastar. We investigate the constraints on parameters at the junction interference with a time-like thin shell in Section **7**. In Section **8**, we obtain the static gravastar solution, and briefly outline the linearized stability analysis with the determined stability regions of the transition layer in Section **9**. We also investigate the stability of the gravastar by using the surface mass of the thin shell, and discuss in detail some interesting observations. Our conclusions are given in Section **10**. Throughout this work, if not explicitly stated otherwise, we use the units of $G=c=1$.

2 Structural equations of Weyl–Guilfoyle charged fluid

This section is devoted to presenting the basis equations governing the dynamical behavior of a cold charged gravitating distribution of a relativistic fluid. The starting point is to revise the Einstein–Maxwell field equations in a four-dimensional spacetime given by

$$G_{\mu\nu}=R_{\mu\nu}-\frac{1}{2}g_{\mu\nu}R=8\pi(T_{\mu\nu}+E_{\mu\nu}), \tag{1}$$

and,

$$\nabla_\nu F^{\mu\nu}=4\pi J^\mu, \tag{2}$$

$$\nabla_{[\alpha}F_{\mu\nu]}=0 \tag{3}$$

where $R_{\mu\nu}$ is the Ricci tensor, R is the Ricci scalar, and $T_{\mu\nu}$ is the energy–momentum tensor, for which we assume it is a perfect fluid:

$$T_{\mu\nu}=(\rho_m+p)U_\mu U_\nu+pg_{\nu\mu}, \tag{4}$$

where ρ_m is the energy density, p is the isotropic fluid pressure, and U_μ is the 4–velocity of the relativistic

matter fluid. Also, $E_{\mu\nu}$ is the energy tensor of the electromagnetic field, given by

$$E_{\mu\nu}=\frac{1}{4\pi}\left(F_{\mu}^{\lambda}F_{\nu\lambda}-\frac{1}{4}g_{\mu\nu}F_{\lambda\sigma}F^{\lambda\sigma}\right), \tag{5}$$

with $F_{\mu\nu}$ representing the electromagnetic field-strength tensor, given by

$$F_{\mu\nu}=\partial_{\mu}A_{\nu}-\partial_{\nu}A_{\mu}, \tag{6}$$

where $A^{\mu}=\left(\phi,\vec{A}\right)$ is the electromagnetic 4–potential. Finally, with $\rho_{\rm e}$ denoting the associated density of electric charges, the 4–current density can be expressed as

$$J_{\mu}=\rho_{\rm e}U_{\mu}, \tag{7}$$

whose temporal component J^0 is equal to the charge density $\rho_{\rm e}$, and whose spatial components J^i are just the usual 3–vector current components. A static spherically symmetric spacetime is described by the line element

$$\mathrm{d}s^2=g_{\mu\nu}\mathrm{d}x^{\mu}\mathrm{d}x^{\nu}, \tag{8}$$

which can be rewritten in the form

$$\mathrm{d}s^2=-W^2\mathrm{d}t^2+h_{ij}\mathrm{d}x^i\mathrm{d}x^j, \tag{9}$$

where W is the gravitational potential, so the 4–potential A_{μ} and the 4–velocity U_{μ} are defined via

$$A_{\mu}=-\phi\delta_{\mu}^{0}, \qquad \text{and} \quad U_{\mu}=-W\delta_{\mu}^{0}. \tag{10}$$

Notice that we are considering only pure electric fields $A_{\mu}=(-\phi,0,0,0)$, and also, h_{ij} are functions of the spatial coordinates x^i only with $i=1,2,3$. In particular, we are interested in a class of the Guilfoyle solutions [27, 29] where the gravitational potential W and the electric potential ϕ are related by means of the equation

$$W(\phi)=\sqrt{a(b-\epsilon\phi)^2+b_1}, \tag{11}$$

where a, b and b_1 are arbitrary constant and $\epsilon=\pm1$. Here the parameter a is the *Guilfoyle parameter*. As stated in Ref. [28], from the set of quantities $\{\rho_m,p,\rho_{\rm e},\rho_{em}\}$ we obtain the following equation of state:

$$p=\frac{a(b-\epsilon\phi)\rho_{\rm e}-\epsilon W(\phi)\left[\rho_m+(1-a)\rho_{em}\right]}{3\epsilon W(\phi)}, \tag{12}$$

where ρ_{em} is the electromagnetic energy density defined by means of the Weyl–Guilfoyle relation:

$$\rho_{em}=\frac{1}{8\pi}\frac{(\nabla_i\phi)^2}{W^2(\phi)}. \tag{13}$$

3 Spherical equations: general analysis

The geometry of the static spherically symmetric solution for a charged fluid distribution found by Guilfoyle [27] can be written in the usual Schwarzschild coordinates, (t,r,θ,φ) as

$$\mathrm{d}s^2=-N(r)\mathrm{d}t^2+B(r)\mathrm{d}r^2+r^2\left(\mathrm{d}\theta^2+\sin^2\theta\mathrm{d}\varphi^2\right), \tag{14}$$

where the structural functions N and B depend on the radial coordinate r only, so the gauge field and 4–velocity are then given by

$$A_{\mu}=-\phi\delta_{\mu}^{0}, \qquad \text{and} \qquad U_{\mu}=-\sqrt{N(r)}\delta_{\mu}^{0}. \tag{15}$$

We now turn our attention to the stellar mass equation of the spherically symmetric solutions due to the total contribution of the matter energy density and electric energy density. Thus, the mass inside a sphere of radius r can be obtained from the following relation:

$$M(r)=4\pi\int_0^r\left(\rho_m(r)+\frac{Q^2}{8\pi r^4}\right)r^2\mathrm{d}r+\frac{Q^2}{2r}, \tag{16}$$

and therefore, the total charge enclosed in the same region becomes

$$Q(r)=4\pi\int_0^r\rho_{\rm e}(r)\sqrt{B(r)}r^2\mathrm{d}r. \tag{17}$$

Our main goal here is to study a type of system for which the lapse function $N(r)$ connects the gravitational and electric potentials via the Majumdar–Papapetrou relation $N(r)=W^2(\phi(r))=a[b-\epsilon\phi(r)]^2$ ($b_1=0$ in Eq. (11)), in which case one gets

$$\epsilon\phi(r)=b-\sqrt{\frac{N(r)}{a}}. \tag{18}$$

Due to the additive nature of the fields, the constant b can be absorbed into the potential, so without loss of generality we choose $b=0$ and the lapse function becomes

$$N(r)=a[\epsilon\phi(r)]^2=a\phi(r)^2. \tag{19}$$

For static spherically symmetric configurations, as considered in the present research, we have written only the components of tt and rr of the Einstein equation (1), giving the following relations [28, 29]:

$$\frac{1}{rB(r)}\frac{\mathrm{d}}{\mathrm{d}r}\ln[N(r)B(r)]=8\pi(\rho_m(r)+p(r)), \tag{20}$$

$$\frac{\mathrm{d}}{\mathrm{d}r}\left[\frac{r}{B(r)}\right]=8\pi\left(\rho_m(r)+\frac{Q^2}{8\pi r^4}\right), \tag{21}$$

whereas the first integral of the only nonzero component of Maxwell's equations (2) gives

$$Q(r)=\frac{r^2\phi'(r)}{\sqrt{N(r)B(r)}}, \tag{22}$$

where an integration constant is set to zero and a prime denotes a derivative with respect to the radial coordinate r. Therefore, by making use of Eq. (19) in Eq. (22), we obtain a differential form for the electric charge,

$$Q(r)=-\frac{\epsilon}{2\sqrt{a}}\frac{r^2N'(r)}{\sqrt{B(r)}N(r)}. \tag{23}$$

Therefore, one can easily obtain the electric charge inside a spherical surface of radius r, if the metric functions are known. Finally, the conservation law $\nabla_{\mu}T^{\mu\nu}=0$ together

with Maxwell's equations leads to the hydrostatic equilibrium equation that determines the global structure of an electrically charged star by requiring the conservation of mass-energy [32, 33] for the system:

$$2p'(r)+\frac{N'(r)}{N(r)}[\rho_m(r)+p(r)]-2\frac{\phi'(r)\rho_{\rm e}(r)}{\sqrt{N(r)}}=0, \quad (24)$$

which is the only non-identically zero component of the conservation equations. The first two terms on the l.h.s. come from the gravitational force with an isotropic pressure and density, while the second term is due to the Coulomb force that depends on the matter by the metric coefficient.

4 Guilfoyle's solutions for the interior region

In this section we describe a static spherically symetric distribution of electrically charged matter in the range $0\leqslant r\leqslant r_0$. To do this, we adopt the simplest ansatz of Guilfoyle's solution [27] given by

$$8\pi\rho_m+\frac{Q^2}{r^4}=\frac{3}{R^2}, \quad (25)$$

where $r\leqslant r_0$ and R is a constant which characterizes the length associated with the inverse of the total energy density. It can also be related to the parameters of the exterior solution, namely the total charge q and the total mass m evaluated at the junction boundary $r=r_0$,

$$\frac{1}{R^2}=\frac{2}{r_0^3}\left(m-\frac{q^2}{2r_0}\right), \quad (26)$$

where

$$m=M(r_0)=4\pi\int_0^{r_0}\left(\rho_m(r)+\frac{Q^2}{8\pi r^4}\right)r^2\,{\rm d}r+\frac{q^2}{2r_0}. \quad (27)$$

$$q=Q(r_0). \quad (28)$$

Using this additional assumption, Guilfoyle [27] found the exact solutions of the Einstein–Maxwell equations, which can be summarized as follows. The structural functions become

$$B(r)=1-\frac{r^2}{R^2}, \quad (29)$$

$$N(r)=\left[\frac{(2-a)}{a}F(r)\right]^{\frac{2a}{(a-2)}}, \quad (30)$$

with the function $F(r)$ defined as

$$F(r)=c_o\sqrt{1-\frac{r^2}{R^2}}-c_1, \quad (31)$$

where the integration constants c_0 and c_1, obtained via the junction conditions, are given by

$$c_0=\frac{R^2}{r_0^2}\left(\frac{m}{r_0}-\frac{q^2}{r_0^2}\right)\left(1-\frac{r_0^2}{R^2}\right)^{-1/a}, \quad (32)$$

$$c_1=c_0\sqrt{1-\frac{r_0^2}{R^2}}\left[1-\frac{a}{(2-a)}\frac{r_0^2}{R^2}\left(\frac{m}{r_0}-\frac{q^2}{r_0^2}\right)^{-1}\right]. \quad (33)$$

Thus, from Eq. (19), the electric potential is given by

$$\phi(r)=\frac{\epsilon}{\sqrt{a}}\left[\frac{(2-a)}{a}F(r)\right]^{\frac{a}{(a-2)}}, \quad (34)$$

whereas the fluid quantities are given by

$$8\pi\rho_m(r)=\frac{3}{R^2}\left[1-\frac{ac_0^2}{3R^2(2-a)^2}\frac{r^2}{F^2(r)}\right], \quad (35)$$

$$8\pi p(r)=-\frac{1}{R^2}\left[1+\frac{ac_0^2}{R^2(2-a)^2}\frac{r^2}{F^2(r)}+-\frac{2a}{(2-a)}\frac{F(r)+c_1}{F(r)}\right], \quad (36)$$

$$8\pi\rho_{\rm e}(r)=\frac{\epsilon\sqrt{a}}{R^4(2-a)}\frac{r^2}{F^2(r)}\left[c_0^2+\frac{3F(r)(F(r)+c_1)}{r^2}\right]. \quad (37)$$

Finally, inserting the above relations into Eqs. (16) and (17), the mass and electric charge functions $M(r)$ and $Q(r)$ are found to be

$$M(r)=\frac{r^3}{2R^2}\left[1+\frac{ac_0^2}{R^2(2-a)^2}\frac{r^2}{F^2(r)}\right], \quad (38)$$

and

$$Q(r)=\frac{\epsilon\sqrt{a}c_0}{R^2(2-a)}\frac{r^3}{F(r)}, \quad (39)$$

respectively.

5 Review of gravastar models

This section presents a quick review of the main features of two gravastar models, which have some interesting properties for our subsequent study.

5.1 Mazur–Mottola model

The first model presented here is the so–called *Mazur & Mottola gravastar model* [6]. According to this model, the interior of the gravastar is a de Sitter spacetime surrounded by a layer of ultra–stiff matter, while the exterior is then suitably matched by a Schwarzschild spacetime i.e., there are five different regions (including two thin shells), each with its own features:

1) Inside the gravastar $0\leqslant r<r_1$, a de Sitter spacetime with $p=-\rho$.

2) An interior thin shell at $r_1\lesssim r_s$ with surface density σ_- and surface tension ϑ_-.

3) A finite layer of ultra–stiff matter, $p=\rho$, placed at $r_1<r<r_2$.

4) An exterior thin shell at $r_2\gtrsim r_s$ with surface density σ_+ and surface tension ϑ_+.

5) An exterior Schwarzschild vacuum $r>r_2$ with $p=\rho=0$.

These features are the most important for a gravastar model having negative central pressure, positive density and the absence of event and cosmological horizons. Notice that here ρ is the energy density and p is the isotropic pressure of the gravastar, whereas the interior has a constant energy density given by $\rho_{\rm int}=3H_0^2/8\pi\geqslant 0$. From a physical point of view, region (3) is the most important because that is where the non–trivial model for the gravastar can be specified.

5.2 The thin–shell gravastar model

The second model to be reviewed is the *Visser & Wiltshire gravastar model* [9], in which the authors tried to determine the possibility of dynamically testing the stability of the gravastar model against radial perturbations. In this sense, the scenario allows a precise formation mechanism, in which the number of layers of the original model is reduced from five to three. Therefore, the most important features of the model are:

1) Inside the gravastar, $r<r_0$, a de Sitter spacetime with $p=-\rho$ is assumed, together with the strong condition $\rho>0$.

2) The spacetime is assumed to be free of singularities everywhere. In order to avoid both event and cosmological horizons, a single thin shell with a surface density σ and surface tension ϑ is placed at $r=a\gtrsim r_s$.

3) The interior spacetime is matched to the exterior vacuum at the junction interface Σ situated at $r=a$.

A particular illustration in this model that offers a de Sitter interior solution was matched smoothly to the exterior Schwarzschild geometry at a junction surface, composed of a thin shell with surface energy density σ and surface pressure $\mathcal{P}$. Using this technique, we obtain a condition for dynamical stability for the thin shell against radial perturbations in terms of a thin shell's equation of motion given by $\frac{1}{2}\dot{a^2}+V(a)=0$, with $\mathrm{R}\equiv\frac{\mathrm{d}R}{\mathrm{d}\tau}$ and τ being the proper time of the timelike hypersurface. In this context, we perform a similar procedure outlined by Visser & Wiltshire and analyze the stability of gravastars against radial perturbations.

6 Construction of gravastar model

This section is devoted to modelling a specific gravastar geometry by matching an interior de Sitter spacetime with an exterior Reissner–Nordström spacetime at a junction interface Σ. So, the structural functions $N(r)$ and $B(r)$ are given by

$$N(r)=B(r)^{-1}=\begin{cases}1-\dfrac{r^2}{R^2} & \text{when } r<a(\tau),\\[2ex] 1-\dfrac{2m}{r}+\dfrac{q^2}{r^2} & \text{when } r>a(\tau),\end{cases}\tag{40}$$

where $r=a(\tau)$ is the timelike hypersurface at which the infinitely thin shell is located at the proper time τ. Now we focus on the analysis of the separating surface between the two spacetimes, which is defined by the radial coordinate $r_0=a(\tau)$. In the procedure of matching the interior de Sitter spacetime to the exterior Reissner–Nordström spacetime, we must consider two different manifolds: an exterior $\mathcal{V}^+$ and an interior $\mathcal{V}^-$, which are joined at the surface layer Σ, and induce the metrics g_{ij}^+ and g_{ij}^-, respectively. Thus, a single manifold $\mathcal{V}=\mathcal{V}^+\cup\mathcal{V}^-$ is obtained by gluing them together at their boundaries. The induced metric on the hypersurface is a timelike hypersurface Σ, defined by a parametric equation in the form $f(x^\mu(\xi^i))=0$, where $\xi^i=(\tau,\theta,\varphi)$ denotes the intrinsic coordinates on Σ. In order to describe the position of the junction surface, we consider $\xi^\mu(\tau,\theta,\varphi)=(t(\tau),a(\tau),\theta,\varphi)$, and the induced metric on the hypersurface can be written as

$$\mathrm{d}s^2=-\mathrm{d}\tau^2+a^2(\tau)\mathrm{d}\Omega_2^2,\tag{41}$$

where τ is the proper time along the hypersurface Σ.

Next, we use the Darmois–Israel formalism to determine the relation between the geometry and thin layer of matter at the shell across a junction surface, which is given by the Lanczos equations [10, 34]:

$$S_j^i=-\frac{1}{8\pi}\left(\kappa_j^i-\delta_j^i\kappa_m^m\right),\tag{42}$$

where S_{ij} represents the surface energy–momentum tensor and the discontinuity in the second fundamental form or extrinsic curvatures across a junction surface is given by the quantity $\kappa_{ij}=K_{ij}^+-K_{ij}^-$, which is associated with both sides of the shell. Also, the extrinsic curvature $K_{ij}^\pm$ is defined on each side of the shell, and is given by

$$K_{ij}^\pm=-\eta_\nu^\pm\left(\frac{\partial^2x^\nu}{\partial\xi^i\partial\xi^j}+\Gamma_{\alpha\beta}^{\nu\pm}\frac{\partial x^\alpha}{\partial\xi^i}\frac{\partial x^\beta}{\partial\xi^j}\right),\tag{43}$$

where η_ν represents the unit normal vector to Σ and ξ^i represents the intrinsic coordinates. Thus, at the hypersurface Σ, whose parametric equation is given by $f(x^\mu(\xi^i))=0$, the respective unit 4–normal vectors $\eta_\nu^\pm$ to Σ are

$$n_\mu^\pm=\pm\left|g^{\alpha\beta}\frac{\partial f}{\partial x^\alpha}\frac{\partial f}{\partial x^\beta}\right|^{-\frac{1}{2}}\frac{\partial f}{\partial x^\mu},\tag{44}$$

where the unitary conditions $n_\mu n^\mu=+1$ and $n_\mu \mathrm{e}_{(i)}^\mu=0$ are oriented outwards from the origin. By using Eq. (44), normal vectors may be determined from the interior and

exterior spacetimes given in Eq. (40), so they become

$$n^{\mu}_{-}=\left(\frac{\dot{a}}{\left(1-\frac{a^2}{R^2}\right)},\sqrt{\left(1-\frac{a^2}{R^2}\right)+\dot{a}^2},0,0\right), \quad (45)$$

$$n^{\mu}_{+}=\left(\frac{\dot{a}}{1-\frac{2M}{a}+\frac{q^2}{a^2}},\sqrt{1-\frac{2M}{a}+\frac{q^2}{a^2}+\dot{a}^2},0,0\right), \quad (46)$$

where the $(\pm)$ superscripts correspond to the exterior and interior spacetimes, respectively.

The discontinuity of the extrinsic curvature κ_{ij} can be written in a simple form due to spherical symmetry as $\kappa^i_j=\mathrm{diag}(\kappa^{\tau}_{\tau},\kappa^{\theta}_{\theta},\kappa^{\theta}_{\theta})$, with $\kappa^{\theta}_{\theta}=\kappa^{\varphi}_{\varphi}$. By employing the expressions through Eq. (42), we find the non–vanishing components of surface stress–energy tensor that can be written in terms of $S^i_j=\mathrm{diag}(-\sigma,\mathcal{P},\mathcal{P})$, where σ is the surface energy density and P is the surface pressure.

Now, using Eq. (40) and Eq. (43), the non–trivial components of the extrinsic curvature are given by

$$K^{\theta-}_{\theta} = \frac{1}{a}\sqrt{\left(1-\frac{a^2}{R^2}\right)+\dot{a}^2}, \quad (47)$$

$$K^{\tau-}_{\tau} = \frac{\left(\ddot{a}-\frac{a}{R^2}\right)}{\sqrt{\left(1-\frac{a^2}{R^2}\right)+\dot{a}^2}}, \quad (48)$$

$$K^{\theta+}_{\theta} = \frac{1}{a}\sqrt{1-\frac{2M}{a}+\frac{q^2}{a^2}+\dot{a}^2}, \quad (49)$$

$$K^{\tau+}_{\tau} = \frac{\ddot{a}+\frac{M}{a^2}-\frac{q^2}{a^3}}{\sqrt{1-\frac{2M}{a}+\frac{q^2}{a^2}+\dot{a}^2}}, \quad (50)$$

where dots denote the derivatives with respect to τ. Therefore, using Eqs. (47, 48, 49, 50) in the Lanczos equations (42), we find that the energy density $\sigma\equiv-\kappa^{\theta}_{\theta}/4\pi$ and the pressure at the junction surface $\mathcal{P}\equiv(\kappa^{\tau}_{\tau}+\kappa^{\theta}_{\theta})/8\pi$ become

$$\sigma=-\frac{1}{4\pi a}\left[\sqrt{1-\frac{2M}{a}+\frac{q^2}{a^2}+\dot{a}^2}-\sqrt{1-\frac{a^2}{R^2}+\dot{a}^2}\right], \quad (51)$$

and

$$\mathcal{P}=\frac{1}{8\pi a}\left[\frac{1-\frac{M}{a}+\dot{a}^2+a\ddot{a}}{\sqrt{1-\frac{2M}{a}+\frac{q^2}{a^2}+\dot{a}^2}}-\frac{1-\frac{2a^2}{R^2}+\dot{a}^2+a\ddot{a}}{\sqrt{1-\frac{a^2}{R^2}+\dot{a}^2}}\right], \quad (52)$$

respectively. Notice that the surface density σ has the opposite sign to the surface pressure $\mathcal{P}$, and also that all the energy–momentum that plunges into the thin shell still satisfies an energy conservation law, $\nabla_i S^{ij}=0$, by virtue of $\nabla^i(\kappa^{ij}-\delta_{ij}\kappa)=0$ at the junction interface.

Now, using two equations, Eqs. (51) and (52), it is easy to check the energy conservation equation is fulfilled:

$$\frac{\mathrm{d}}{\mathrm{d}\tau}(\sigma a^2)+\mathcal{P}\frac{\mathrm{d}}{\mathrm{d}\tau}(a^2)=0, \quad (53)$$

from which immediately follows

$$\dot{\sigma}=-2(\sigma+\mathcal{P})\frac{\dot{a}}{a}. \quad (54)$$

Integrating out the above equation, it yields

$$\sigma'=-\frac{2}{a}(\sigma+\mathcal{P}), \quad (55)$$

where primes and dots denote differentiation with respect to a and τ, respectively. The first term on the left side of Eq. (53) represents the internal energy change of the shell, while the work done by internal forces of the shell is given in the second term.

Now, by taking into account Eqs. (51-52) and substituting into Eq. (55), we obtain the following expression,

$$\sigma'=\frac{1}{4\pi a^2}\left[\frac{1-\frac{3M}{a}+\frac{2q^2}{a^2}+\dot{a}^2-a\ddot{a}}{\sqrt{1-\frac{2M}{a}+\frac{q^2}{a^2}+\dot{a}^2}}-\frac{1+\dot{a}^2-a\ddot{a}}{\sqrt{1-\frac{a^2}{R^2}+\dot{a}^2}}\right], \quad (56)$$

which plays an important role in determining the stability regions when the static solution a_0 is being considered.

According to Refs. [35, 36], the total surface mass of the thin shell is given by $m_s=4\pi a^2\sigma$. For this case the total mass of the system M evaluated at a static solution a_0 is given by (by rearranging Eq. (51))

$$M=\frac{a_0^3}{2R^2}+\frac{q^2}{2a_0}+m_s\left[\sqrt{1-\frac{a_0^2}{R^2}}-\frac{m_s(a_0)}{2a_0}\right]. \quad (57)$$

Note that $M(a)$ is the total active gravitational mass and $q(a)^2/2a$ is the mass equivalent to the electromagnetic field.

7 Junction conditions

Keep in mind that a gravastar model does not possess an event horizon. For instance, if the thin–shell transition layer Σ is located at $r=a(\tau)$, then to avoid horizon formation we demand

$$0<\left|\frac{r}{R}\right|<1 \ \text{ and } \ 0<\left|\frac{2M}{r}-\frac{q^2}{r^2}\right|<1. \quad (58)$$

For the present analysis, one can obtain the solution of the non–rotating thin shell gravastar when the spacetimes given by the metrics (40) are matched at a. The restriction of charge–to–mass ratio $|q|/M<1$ for the Reissner-Nordström spacetime corresponds to two

horizons, namely the Cauchy and event horizons $r_\pm = M\left(1\pm\sqrt{1-q^2/M^2}\right)$. When $|q|/M\to 1$, these are glued into a single horizon. For the case when $|q|/M>1$, it is a naked singularity. Moreover, we consider the case when $|q|/M\leqslant 1$ in order to avoid the horizon from geometry, where $a>r_+=M\left(1+\sqrt{1-q^2/M^2}\right)$. We develop the rest of the section by assuming $|q|/M\leqslant 1$, where the junction surface $r=a$ is situated outside the event horizon.

8 Static gravastars

Now, we resolve the static case, which is given by $\dot{a}=\ddot{a}=0$. In this case, Eqs. (51) and (52) reduce to

$$\sigma(a_0)=-\frac{1}{4\pi a_0}\left[\sqrt{1-\frac{2M}{a_0}+\frac{q^2}{a_0^2}}-\sqrt{1-\frac{a_0^2}{R^2}}\right], \tag{59}$$

$$\mathcal{P}(a_0)=\frac{1}{8\pi a_0}\left[\frac{1-\frac{M}{a_0}}{\sqrt{1-\frac{2M}{a_0}+\frac{q^2}{a_0^2}}}-\frac{1-\frac{2a_0^2}{R^2}}{\sqrt{1-\frac{a_0^2}{R^2}}}\right]. \tag{60}$$

It is worth noting that the gravastar solution is also considered a self-gravitating object, which can avoid the formation of the black hole horizon. Hence, a gravastar model can be considered as one type of compact object where the surface redshift is an important source of information. We expect that the redshifts of gravastars would be higher than any ordinary objects. The surface gravitational redshift is defined by $z=\Delta\lambda/\lambda_{\rm e}=\lambda_0/\lambda_{\rm e}$, where Δ is the fractional change between the observed wavelength λ_0 and the emitted wavelength $\lambda_{\rm e}$.

Thus, in our notation, the redshift factor z_{a_0} is

$$z_{a_0}=-1+\left|g_{tt}(a_0)\right|^{-1/2}, \tag{61}$$

Now, the behavior of the surface redshift is not larger than $z=2$ [37] for a static perfect fluid sphere. This value may increase up to 3.84, when we consider anisotropic fluid spheres [38].

In order to specify an equilibrium solution for the thin–shell gravastar, we introduce the dimensionless configuration variables defined by Ref. [39],

$$x\equiv\frac{M}{a_0},\qquad y\equiv\frac{M}{R},\quad\text{and}\qquad w\equiv\frac{q}{M}. \tag{62}$$

Therefore, assuming the condition of $|q|<a_0<R$, the surface energy density $\sigma(a_0)=\sigma(x)$ and the surface pressure $\mathcal{P}(a_0)=\mathcal{P}(x)$ can be written as

$$\sigma(x)=-\frac{1}{4\pi R}\frac{x}{y}\left(\sqrt{1-2x+w^2x^2}-\sqrt{1-\frac{y^2}{x^2}}\right), \tag{63}$$

and

$$\mathcal{P}(x)=\frac{1}{8\pi R}\frac{x}{y}\left(\frac{1-x}{\sqrt{1-2x+w^2x^2}}-\frac{1-2\frac{y^2}{x^2}}{\sqrt{1-\frac{y^2}{x^2}}}\right). \tag{64}$$

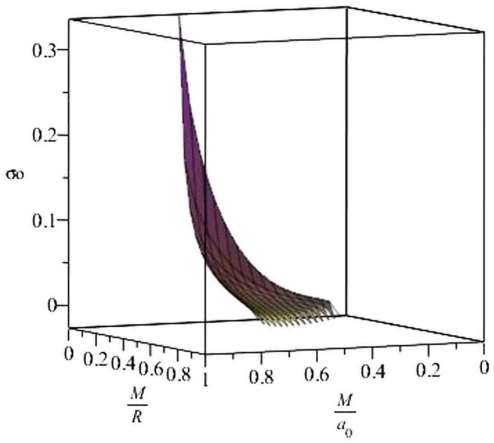

Fig. 1. Unification diagram for surface energy density $\sigma(a_0)$. We have considered the dimensionless parameters $x=M/a_0$ and $y=M/R$. The qualitative values used for drawing the graphs are $w=0.5$ and $R=3$. Note that surface energy density and surface pressure are both positive in the range. See the Appendix for more details.

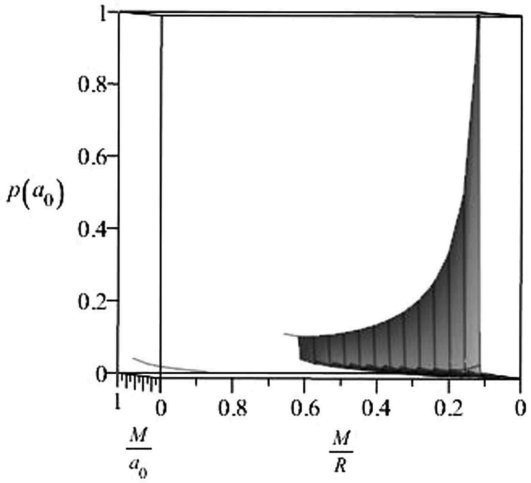

Fig. 2. Surface pressure, with $w=0.5$ and $R=3$ used as the values of the parameters for graphical representation.

9 Linearized stability of gravastars

In this section we study the stability of the gravastar model about the static solutions a_0, also known as

the linearized stability of the solutions. In order to test whether the equilibrium solution is stable or not, we rearrange Eq. (51) in the following suggestive form,

$$\frac{1}{2}\dot{a}^2+V(a)=0, \tag{65}$$

which is known as the thin–shell equation of motion, with the effective potential given by

$$V(a)=-\frac{256\sigma^4(a)\pi^4a^4-32\pi^2a^2\sigma^2(a)\Xi(a)+\zeta^2(a)}{64\sigma^2(a)\pi^2a^2}, \tag{66}$$

where, for computational convenience, we introduce the functions $\Xi(a)$ and $\zeta(a)$ with the following definitions:

$$\Xi(a) = \left(1-\frac{2M}{a}+\frac{q^2}{a^2}\right)+\left(1-\frac{a^2}{R^2}\right), \tag{67}$$

$$\zeta(a) = \left(1-\frac{2M}{a}+\frac{q^2}{a^2}\right)-\left(1-\frac{a^2}{R^2}\right). \tag{68}$$

This allows us to write the potential in a second-order differential form as

$$V''(a)=\frac{1}{32\sigma^4a^4\pi^2}\left[\Delta_1\sigma''+16\sigma^4\pi^2\Xi''a^4-\sigma^2\zeta a^2\zeta''+\Delta_2\sigma'+\Delta_3(\sigma')^2-256\sigma^6\pi^4a^4-\sigma^2\zeta'^2a^2+4\sigma^2\zeta'\zeta a-3\sigma^2\zeta^2\right], \tag{69}$$

where

$$\begin{aligned}\Delta_1 &= -256a^6\pi^4\sigma^5+a^2\zeta^2\sigma,\\ \Delta_2 &= -1024a^5\pi^4\sigma^5+4a^2\sigma\zeta\zeta'-4a\zeta^2\sigma,\\ \Delta_3 &= -256a^6\pi^4\sigma^4-3a^2\zeta^2.\end{aligned}$$

In the study of the stability of a static solution at a_0, we perform a Taylor expansion of $V(a)$ about a_0 until second–order terms, given by

$$V(a) = V(a_0)+V'(a_0)(a-a_0)+\frac{1}{2}V''(a_0)(a-a_0)^2+O[(a-a_0)^3], \tag{70}$$

where a prime denotes the derivative with respect to a. Here we adapt and apply the criteria for stability analysis of a static configuration at $a=a_0$, which requires $V(a_0)=V'(a_0)=0$. The condition for stability is that $V''(a_0)>0$, to guarantee that the second derivative of the potential is positive. In order to determine the stability of the gravastar we first calculate $V''(a_0)$. Using Eq. (55) and by introducing a new parameter $\eta_0=\mathcal{P}'(a_0)/\sigma'(a_0)$ into Eq. (69), we obtain

$$\begin{aligned}V''(a_0) = \frac{1}{32\pi^2\sigma_0^4a_0^8R^4}\Bigg\{&-1024\left(\eta_0+\frac{3}{4}\right)\pi^4R^4a_0^8\sigma_0^6-1024\sigma_0^5\pi^4R^4a_0^8\left(\eta_0+\frac{3}{2}\right)p_0\\ &-64\left[\left(16a_0^4p_0^2\pi^2+Ma_0-\frac{3}{2}q^2\right)R^2+\frac{1}{2}a_0^4\right]\pi^2R^2a_0^4\sigma_0^4-48p^2\left[\left(Ma_0-\frac{1}{2}q^2\right)R^2-\frac{a_0^4}{2}\right]^2\\ &+16p\left[\left(M\left(\eta_0-\frac{1}{2}\right)a_0-\frac{1}{2}q^2\left(\eta_0+\frac{3}{2}\right)\right)R^2-1/2\left(\eta_0-\frac{13}{2}\right)a_0^4\right]\left[\left(Ma_0-\frac{q^2}{2}\right)R^2-\frac{a_0^4}{2}\right]\sigma_0\\ &+\left[\left(16M^2a_0^2\eta_0-16Mq^2\left(\eta_0-\frac{1}{4}\right)a_0+4\left(\eta_0-\frac{3}{4}\right)q^4\right)R^4-16\left(M\left(\eta_0-\frac{3}{4}\right)a_0-\frac{1}{2}q^2\left(\eta_0-\frac{1}{4}\right)\right)a_0^4R^2\right.\\ &\left.+4\left(\eta_0-\frac{15}{4}\right)a_0^8\right]\sigma_0^2\Bigg\}.\end{aligned} \tag{71}$$

Therefore, by demanding that $V''(a_0)>0$, we find an inequality for the η_0 parameter, which yields

$$\eta_0>\frac{768\sigma_0^6\pi^4R^4a_0^8+1536\sigma_0^5\pi^4R^4a_0^8p_0+64\pi^2R^2a_0^4\sigma_0^4\Theta_1+\sigma_0^2\Theta_2+8\pi\sigma a_0\Theta_3+48p_0^2\Theta_4}{4\sigma_0(\sigma_0+p_0)(-256\sigma_0^4\pi^4a_0^8R^4+4M^2a_0^2R^4-4Ma_0R^4q^2-4Ma_0^5R^2+R^4q^4+2a_0^4R^2q^2+a_0^8)}, \tag{72}$$

$$\text{if}\qquad \sigma_0(\sigma_0+p_0)(-256\sigma_0^4\pi^4a_0^8R^4+4M^2a_0^2R^4-4Ma_0R^4q^2-4Ma_0^5R^2+R^4q^4+2a_0^4R^2q^2+a_0^8)>0,$$

and

$$\eta_0<\frac{768\sigma_0^6\pi^4R^4a_0^8+1536\sigma_0^5\pi^4R^4a_0^8p_0+64\pi^2R^2a_0^4\sigma_0^4\Theta_1+\sigma_0^2\Theta_2+8\pi\sigma a_0\Theta_3+48p_0^2\Theta_4}{4\sigma_0(\sigma_0+p_0)(-256\sigma_0^4\pi^4a_0^8R^4+4M^2a_0^2R^4-4Ma_0R^4q^2-4Ma_0^5R^2+R^4q^4+2a_0^4R^2q^2+a_0^8)}, \tag{73}$$

$$\text{if}\qquad \sigma_0(\sigma_0+p_0)(-256\sigma_0^4\pi^4a_0^8R^4+4M^2a_0^2R^4-4Ma_0R^4q^2-4Ma_0^5R^2+R^4q^4+2a_0^4R^2q^2+a_0^8)<0.$$

For notational simplicity, in Eqs. (72) and (73), we use

$$\Theta_1 = \left(16a_0^4p_0^2\pi^2+Ma_0-\frac{3q^2}{2}\right)R^2+\frac{a_0^4}{2},$$

$$\Theta_2 = (-4Ma_0q^2+3q^4)R^4+2a_0^4(q^2-6Ma_0)R^2+15a_0^8,$$

$$\Theta_3 = \left[\left(Ma_0+\frac{3q^2}{2}\right)R^2-\frac{13a_0^4}{2}\right]\left[\left(Ma_0-\frac{q^2}{2}\right)R^2-\frac{a_0^4}{2}\right],$$

$$\Theta_4 = \left[\left(Ma_0-\frac{q^2}{2}\right)R^2-\frac{a_0^4}{2}\right]^2.$$

Obviously, to ensure stability, we demand that in equilibrium the configurations satisfy the usual condition $V''(a_0)>0$. To justify our assumption for a given set of parameters and find the range of a_0 for which $V''(a_0)>0$, we use a graphical representation, due to the complexity of the expression $V''(a_0)$. In Figs. 3, 4, 5, the stable solutions are displayed for different values of q,M and R. From Eqs. (72)–(73), we find that the regions in the $\eta_0\times a_0$ plane where the stability conditions are satisfied.

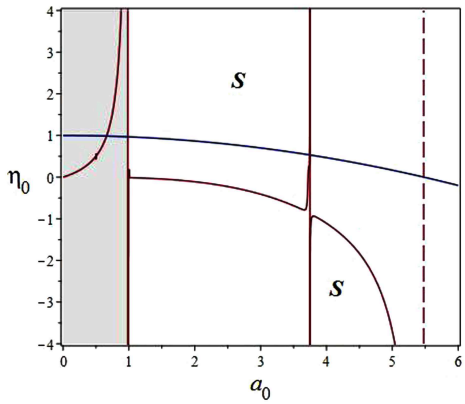

Fig. 3. (color online) Stability regions in terms of η_0 as a function of a_0 for $M=1$ and $q=1$. The shaded region is for $a_0<r_h$, and the dashed vertical line is for $a_0=R$.

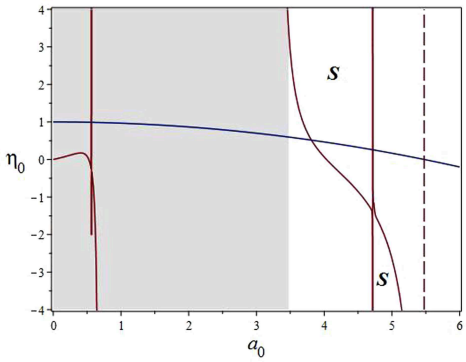

Fig. 4. (color online) Stability regions in terms of η_0 as a function of a_0 for $M=2$ and $q=1.5$. The shaded region is for $a_0<r_h$ and the dashed vertical line is for $a_0=R$.

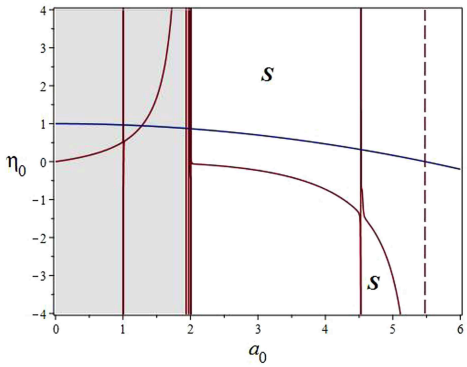

Fig. 5. (color online) Stability regions in terms of η_0 as a function of a_0 for $M=2$ and $q=2$. The shaded region is for $a_0<r_h$ and the dashed vertical line is for $a_0=R$.

To illustrate the above stability conditions, we use η_0 as a parameter so that there is no need to specify any surface equation of state. The parameter η_0 is normally interpreted as the speed of sound, which should lie within the limit (0, 1] based on the physical requirement. However, η_0 may lie outside the range of (0, 1] on the surface layer. For an extensive discussion see Refs.[21, 35].

10 Stability analysis using the surface mass of the thin shell

In this section we study the gravastar stability through the surface mass of the thin shell, following Ref. [39], which is given by $m_s=4\pi a^2\sigma$. For the stability analysis, we do not need to introduce a particular parameter; rather, we can simply choose $\sigma(a)$, or equivalently m_s, as an arbitrarily specifiable function that encodes the whole gravastar stability.

For our purpose, in the exterior Reissner-Nordström spacetime, with de Sitter interior geometry, the surface mass of the thin shell for a static configuration is given by

$$m_s(a_0)=-a_0\left[\sqrt{1-\frac{2M}{a_0}+\frac{q^2}{a_0^2}}-\sqrt{1-\frac{a_0^2}{R^2}}\right], \tag{74}$$

while for first–order differentiation we have

$$m_s'(a_0)=\left[\frac{1-\frac{2a_0^2}{R^2}}{\sqrt{1-\frac{a_0^2}{R^2}}}-\frac{1-\frac{M}{a_0}}{\sqrt{1-\frac{2M}{a_0}+\frac{q^2}{a_0^2}}}\right]. \tag{75}$$

For a static shell, one can derive the inequality for $m_s''(a_0)$, which may be used for a stable configuration, as the above expression contains two terms with opposite signs.

Generally, we require that the thin–shell matter satisfies the weak and dominant energy conditions. In this

analysis, we shall adapt the cases of $\sigma>0$, which correspond to positive surface energy densities (see the Appendix for more details). By considering a stable static solution at a_0, we must have:

$$a_0 m_s''(a_0)\geqslant\left\{\frac{\left(\frac{a_0}{R}\right)^2\left[2\left(\frac{a_0}{R}\right)^2-3\right]}{\left(1-\frac{a_0^2}{R^2}\right)^{3/2}}-\frac{\left(\frac{M}{a_0}\right)^2\left[\left(\frac{q}{M}\right)^2-1\right]}{\left(1-\frac{2M}{a_0}+\frac{q^2}{a_0^2}\right)^{3/2}}\right\} \tag{76}$$

Now, from the master equation (76), we mimic the stable equilibrium regions of the respective solutions. To determine the stability regions of this solution, we choose the parameters such that the transition layer is located at some value between $|q|<a_0<R$. Since the explicit form of the inequalities is extremely lengthy, we produce the graphical representation shown in Fig. 6, where the stability regions are represented above this surface. This is in good agreement with our previous results.

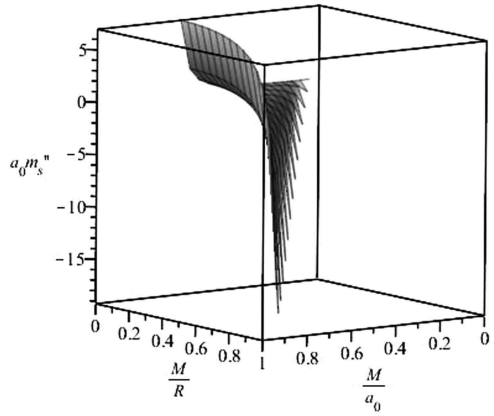

Fig. 6. Plot of the inequality (76) for the function $a_0 m_s''$ in the case that $V=0$. We define the graph for a positive surface energy density and for the values of $q/m<a_0$ and $a_0<R$. The stability regions are given above the surface.

11 Summary and discussion

As an alternative to black holes, compact objects like gravastars have been proposed as a different final state of a gravitational collapse, though the evidence for the existence of black holes is well accepted astrophysically. In this paper, a spherically symmetric charged thin-shell gravastar has been investigated for a certain range of parameters where the metric potentials and electromagnetic fields are related in some particular relation called Guilfoyle's solutions. We consider a gravastar composed of a de Sitter core, a thin shell, and an exterior Reissner-Nordström electrovacuum region.

The most relevant property is that within the δ-shell models surface energy density and surface pressure are positive for a certain range of parameters. Therefore, the obtained solutions satisfy the NEC as illustrated in Fig. 1. For completeness, we have extended our analysis by exploring the linearized spherically symmetric radial perturbations about static equilibrium solutions. In this case, stability regions are given by the plots depicted in Figs. (3,4,5). Furthermore, we have discussed the gravastar stability through the surface mass of the thin shell, and we have show that the obtained results are in good agreement with our previous results. Therefore, we draw the conclusion that a variety of electrically charged gravastar solutions may be constructed from the Guilfoyle exact solutions.

Moreover, when considering charged stars it is useful to examine the mass-radius-charge bounds discussed so far in the literature. However, a separate study is needed for these quantities. Therefore, we plan in the near future to extend our work by considering the mass-radius-charge bounds discussed by Andréasson [40], and Bohmer & Harko [41].

AB is thankful to the authority of Inter-University Centre for Astronomy and Astrophysics, Pune, India for providing research facilities.

Appendix: static gravastars

We derive the surface stress-energy tensor in terms of surface energy density σ and surface pressure $\mathcal{P}$, around a stable solution situated at a_0. To see the qualitative behavior depicted in Figs. 1 and 2, let us start with Eqs. (59, 60) and introduce new variables $x=M/a_0$ and $y=M/R$. Then the surface energy density and the surface pressure read, respectively,

$$\begin{aligned}\sigma(a_0) &= -\frac{1}{4\pi a_0}\left[\sqrt{1-\frac{2M}{a_0}+\frac{q^2}{a^2}}-\sqrt{1-\frac{a_0^2}{R^2}}\right]\\ &= -\frac{1}{4\pi R}\frac{x}{y}\left[\sqrt{1-2x+\frac{q^2}{m^2}x^2}-\sqrt{1-\frac{y^2}{x^2}}\right],\end{aligned} \tag{A1}$$

$$\mathcal{P}(a_0) = \frac{1}{8\pi a_0}\left[\frac{1-\frac{M}{a_0}}{\sqrt{1-\frac{2M}{a_0}+\frac{q^2}{a_0^2}}}-\frac{1-\frac{2a_0^2}{R^2}}{\sqrt{1-\frac{a_0^2}{R^2}}}\right]=\frac{1}{8\pi R}\frac{x}{y}\left[\frac{1-x}{\sqrt{1-2x+\frac{q^2}{m^2}x^2}}-\frac{1-\frac{2y^2}{x^2}}{\sqrt{1-\frac{y^2}{x^2}}}\right]. \tag{A2}$$

Note that surface energy density and surface pressure are both positive in their respective ranges.

References

1 S. Chandrasekhar, Mon. Not. R Astron. Soc., **91**: 5 (1931)
2 W. Baade and F. Zwicky, Phys. Rev., **46**: 1 (1934)
3 L.D. Landau, Phys. Z. Sowjetunion, **1**: 285 - 288 (1932)
4 J.R. Oppenheimer and H. Snyder, Phys. Rev., **56**: 455 (1939)
5 R. Penrose, Phys. Rev. Lett., **14**: 57 (1965)
6 P.O. Mazur and E. Mottola, Gravitational Condensate Stars: An Alternative to Black Holes, 2001 Preprint arXiv:gr-qc/0109035
7 P.O. Mazur and E. Mottola, Dark energy and condensate stars: Casimir energy in the large, Proceedings of the Sixth Workshop on Quantum Field Theory Under the Influence of External Conditions, 2004 Preprint arXiv:gr-qc/0405111
8 P.O. Mazur and E. Mottola, Proc. Nat. Acad. Sci., **111**: 9545 (2004)
9 M. Visser and D. L. Wiltshire, Class. Quant. Grav., **21**: 1135-1152 (2004)
10 W. Israel, Nuovo Cim. B, **44**: S10 (1966) 1; Erratum-ibid B, **48**: 463 (1967)
11 N. Bilić, G.B. Tupper and R.D. Viollier, J. Cosmol. Astropart. Phys., **0602**: 013 (2006)
12 F. S. N. Lobo and A. V. B. Arellano, Class. Quant. Grav., **24**: 1069-1088 (2007),
13 A. DeBenedictis, D. Horvat, S. Ilijić, S. Kloster, and K.S. Viswanathan, Class. Quantum Grav., **23**: 2303 (2006)
14 D. Horvat, S. Ilijić and A. Marunovic, Class. Quant. Grav., **26**: 025003 (2009)
15 A.A. Usmani et al, Phys. Lett. B, **701**: 388-392 (2011)
16 R. Chan et al, JCAP, **1110**: 013 (2011)
17 F. S. N. Lobo, Class. Quant. Grav., **23**: 1525 (2006)
18 A. Das et al, Phys. Rev. D, **95**: 124011 (2017)
19 A. Banerjee and S. Hansraj, Eur. Phys. J. C, **76**: 641 (2016)
20 A. Banerjee et al, Eur. Phys. J. C, **76**: 34 (2016)
21 F.S.N. Lobo and R. Garattini, J. High Energ. Phys., **1312**: 065 (2013)
22 Ali Ovgun, Ayan Banerjee, and Kimet Jusufi, Eur. Phys. J. C, **77**: 566 (2017)
23 H. Reissner, Annalen der Phys., **50**: 106 (1916)
24 H. Weyl, Annalen der Phys., **54**: 117 (1917)
25 H. Weyl, Annalen der Phys., **59**: 185 (1919)
26 S. D. Majumdar, Phys. Rev., **72** 390 - 398 (1947)
27 B. S. Guilfoyle, Gen. Rel. Grav., **31**: 1645-1673 (1999)
28 J. P. S. Lemos and V. T. Zanchin, Phys. Rev. D, **80**: 024010 (2009)
29 J. P. S. Lemos and V. T. Zanchin, Phys. Rev. D, **81**: 124016 (2010)
30 J. P. S. Lemos and V.T. Zanchin, Phys. Rev. D, **93**: 124012 (2016)
31 J. P. S. Lemos and V. T. Zanchin, Class. Quant. Grav. , **32**: 135009 (2015)
32 J. R. Oppenheimer and G. M. Volkoff, Phys. Rev., **55** 374 (1939)
33 R.C. Tolman, Phys. Rev., **55**: 364 (1939)
34 P. Musgrave and K. Lake, Class. Quantum Grav., **13**: 1885 (1996)
35 E. Poisson and M. Visser, Phys. Rev. D, **52**: 7318 (1995)
36 F. S. N. Lobo, Class. Quant. Grav., **23**: 1525-1541 (2006)
37 H. A. Buchdahl, Phys. Rev., **116**: 1027 (1959)
38 B. V. Ivanov, Phys. Rev. D, **65**: 104011 (2002)
39 P. Martin–Moruno et al, J. Cosmol. Astropart. Phys., **03**: 034 (2012)
40 H. Andreasson, Commun. Math. Phys., **288**: 715 (2009)
41 C. G. Boehmer and T. Harko, Gen. Rel. Grav., **39**: 757 (2007)